CALCULATIONS OF THE FLAW SIGNAL GENERATED

BY A DIFFERENTIAL EDDY-CURRENT PROBE

S. A. Jenkins
and
J. R. Bowler

University of Surrey
Guildford
Surrey GU2 5XH
England

INTRODUCTION

Differential eddy-current probes are attractive because of their
insensitivity to lift-off effects. By using two similar coils wound in
opposition we have a sensor that detects variations in the magnetic field
along a line joining their centers. The impedance plane response of a
differential probe to a flaw is rather more complicated than the signal from
a single winding probe, but this is a price one must be prepared to pay for
nullifying the lift-off signal.

We have developed a three dimensional probe-flaw model to predict
eddy-current signals based on a volume integral formulation[1]. In extending
the model to deal with differential and other multi-winding probe
configurations, we have taken, as a starting point for this development, a
three coil system suggested recently as a benchmark problem for the
evaluation of electromagnetic numerical modeling codes[2]. The coil
arrangement is larger than would be typical of an NDE probe but the scale
permits controlled and accurate measurements to be made[3,4] as an
independent check on the code predictions. The probe consists of an
air-cored excitation coil 44mm. O/D, 36mm. I/D, enclosing a pair of matched
sensor coils connected in differential mode (Figure 1). A 3mm. thick
dielectric slab separates the base of the coil support from the workpiece.
This slab has no significant effect on the field therefore the excitation
coil has a fixed effective lift-off of 8mm.

Although the benchmark problem examines the probe response due to a
surface slot in a finite conducting slab, we have, instead, computed the
signals due to a similar flaw in a half-space conductor (Figure 2). It is
possible to adapt the present method for finite slab problems but this
introduces edge effect complications that we wish to avoid. Instead we shall
highlight an effective method for calculating the differential signal. This
aspect of the problem is of particular interest because it has proved to be
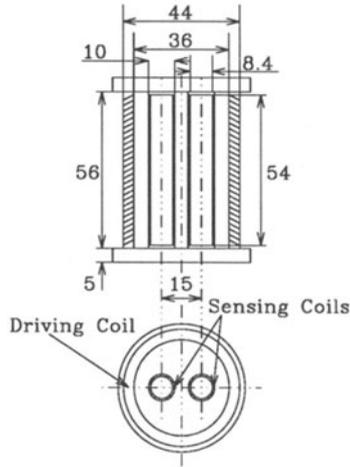very difficult to determine this signal using finite element methods[2].

Review of Progress in Quantitative Nondestructive Evaluation, Vol. 9   **829**
Edited by D.O. Thompson and D.E. Chimenti
Plenum Press, New York, 1990

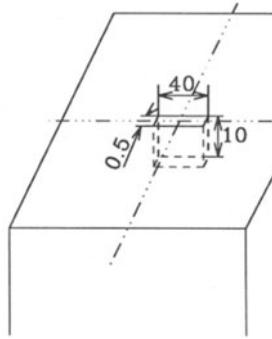Fig. 1. Differential eddy-current probe. Dimensions are in mm.

Fig. 2. Slot in slab of austenitic steel

VOLUME INTEGRAL APPROACH

Assuming the material has a uniform conductivity σ_0 and contains a scatterer of conductivity $\sigma(\bar{r})$, then we define $\bar{P}(\bar{r}) = [\sigma(\bar{r}) - \sigma_0]\bar{E}(\bar{r})$ as the induced electric current dipole moment of the flaw. A formal solution of Maxwell's equations for the electric field in the flawed conductor can then be written as

$$\bar{E}(\bar{r}) = \bar{E}^{(i)}(\bar{r}) + \int_{flaw} \bar{\bar{G}}^{(ee)}(\bar{r}|\bar{r}') \cdot \bar{P}(\bar{r}')d\bar{r}', \tag{1}$$

where $\bar{E}^{(i)}(\bar{r})$ is the incident field and the integral represents the scattered field. In this form we need a dyadic Green's function $\bar{\bar{G}}^{(ee)}(\bar{r}|\bar{r}')$ that transforms the electric source $\bar{P}(\bar{r})$ into an electric field satisfying the correct interface conditions at the surface of the conductor and that vanishes as $|\bar{r}| \to \infty$. An equation for the source distribution $\bar{P}(\bar{r})$ is found by multiplying by $\sigma(\bar{r}) - \sigma_0$ to give,

830

$$\bar{P}(\bar{r}) = \bar{P}^{(i)}(\bar{r}) + v(\bar{r})\sigma_0 \int_{flaw} \bar{G}^{(ee)}(\bar{r}|\bar{r}') \cdot \bar{P}(\bar{r}')d\bar{r}', \qquad (2)$$

where $v(\bar{r}) = [\sigma(\bar{r}) - \sigma_0]/\sigma_0$ and $\bar{P}^{(i)}(\bar{r}) = [\sigma(\bar{r}) - \sigma_0]\bar{E}^{(i)}(\bar{r})$.

An approximate numerical solution of (2) can be found using the method of moments to transform the integral equation into a discrete form[5]. The resulting matrix equation is then solved by applying a conjugate gradient algorithm[6]. This procedure has been used both in calculating the induced magnetisation of the ferrite cores of eddy-current probes[1] and for computing the probe responses due to flaws[7]. Although the discrete representation of (2) requires a dense matrix, the symmetry properties of the Green's function are reflected in the matrix structure which means that we do not have to store every individual element on the computer. For example the free-space Green's function is dependent on $x - x'$, $y - y'$ and $z - z'$, consequently its matrix representation has a Toeplitz structure. In (2), the Green's function can be written as a sum of two terms, one of which is $x - x'$, $y - y'$, $z - z'$ dependent and the other is $x - x'$, $y - y'$, $z + z'$ dependent. (2) therefore contains a combination of convolutional and a correlational integrals. As a result we can develop an approximate matrix representation of the integrals which allows us to perform matrix-vector products using fast Fourier transforms[1].

First the unknown vector, $\bar{P}(\bar{r})$, is expanded in terms of the three-dimensional pulse functions, with cells whose dimensions are δ_x, δ_y and δ_z. Thus,

$$\bar{P}(\bar{r}) = \sum_{k=0}^{N_x-1} \sum_{l=0}^{N_y-1} \sum_{m=0}^{N_z-1} \bar{P}_{klm} P_k(\frac{x}{\delta_x}) P_l(\frac{y}{\delta_y}) P_m(\frac{z-z_0}{\delta_z} - \frac{1}{2}) \ , \qquad (3)$$

where z_0 is the z-coordinate of the lowest level of the flaw region. The pulse function, $P_j(s)$, is defined by

$$P_j(s) = \begin{cases} 1, & \text{if } j - \frac{1}{2} \leq s < j + \frac{1}{2} \\ 0, & \text{otherwise.} \end{cases} \qquad (4)$$

To complete the discretization, the same pulse functions are used for testing. We take moments of the field by multiplying (2) by the pulse functions and then integrating over each cell. This yields a linear system for the solution vector $\bar{P}_{klm}$,

$$\bar{P}_{klm}^{(i)} = \bar{P}_{klm} - v_{klm} \sum_{K=0}^{N_x-1} \sum_{L=0}^{N_y-1} \sum_{M=0}^{N_z-1} \bar{G}_{mM}(k - K, l - L) \cdot \bar{P}_{KLM}, \qquad (5)$$

where the matrix elements are given in terms of the two dimensional Fourier transform of the Green's function $\tilde{G}(z, z')$, by

$$\bar{G}_{mM}(k - K, l - L) = \frac{\delta_x \delta_y \sigma_0}{4\pi^2 \delta_z} \int \int_{-\infty}^{\infty} \tilde{\Upsilon}_{mM}(k_x, k_y) \left[\frac{\sin(k_x \delta_x/2)}{k_x \delta_x/2}\right]^2 \left[\frac{\sin(k_y \delta_y/2)}{k_y \delta_y/2}\right]^2$$
$$\cdot e^{-j[k_x \delta_x(k-K) + k_y \delta_y(l-L)]} \ dk_x \ dk_y. \qquad (6)$$

$\tilde{\Upsilon}_{mM}$ is the result of the integrations with respect to z and z', given by

$$\widetilde{\Upsilon}_{mM}(k_x, k_y) = \int_{z_M}^{z_{M+1}} dz \int_{z_m}^{z_{m+1}} dz' \widetilde{\widetilde{G}}_{(ee)}(z, z'), \tag{7}$$

where $z_m = z_0 + m\delta_z$, $m = 0, 1, \ldots, N_z - 1$.

The incident electric field $\bar{E}^{(i)}(\bar{r})$ has a simple closed form integral Fourier representation for a cylindrical air-cored coil[1]. By taking moments of this form using pulse functions, it is found that the excitation vector $\bar{P}^{(i)}(\bar{r})$ is given by

$$\bar{P}_{klm}^{(i)} = \frac{jnIk^2 v_{klm}}{2\pi\delta_z} \iint_{-\infty}^{\infty} \frac{\rho_2^2 \mathcal{J}(k_r\rho_2) - \rho_1^2 \mathcal{J}(k_r\rho_1)}{k_r \lambda_0 \lambda (\lambda_0 + \lambda)} \cdot \begin{bmatrix} k_y \\ -k_x \\ 0 \end{bmatrix}$$
$$\cdot (e^{-\lambda_0 z_b} - e^{-\lambda_0 z_a})(e^{\lambda z_{k+1}} - e^{\lambda z_k})$$
$$\cdot \frac{\sin(k_x\delta_x/2)}{k_x\delta_x/2} \frac{\sin(k_y\delta_y/2)}{k_y\delta_y/2} e^{-j[k_x(\delta_x k - x_0) + k_y(\delta_y l - y_0)]} dk_x dk_y, \tag{8}$$

where $\lambda_0^2 = k_x^2 + k_y^2 - \omega^2 \mu_0 \epsilon_0$, $\lambda^2 = k_x^2 + k_y^2 - i\omega\mu_0\sigma_0$, z_b and z_a are the top and bottom of the drive coil, ρ_1 and ρ_2 are the inner and outer coil radii, respectively, and

$$\mathcal{J}(s) = \int_0^1 \rho J_1(\rho s) \, d\rho = \frac{2\pi}{s} \left[J_1(s)H_0(s) - J_0(s)H_1(s) \right], \tag{9}$$

where J_0 and J_1 are Bessel functions of the first kind and H_0 and H_1 are Struve functions.

DIFFERENTIAL PROBE RESPONSE

Suppose that the flaw lies in an incident field produced by an excitation coil and that, as a result, there is an induced current dipole density $\bar{P}$ at the flaw. This dipole distribution may be regarded as the source of the scattered electric field, $\bar{E}^{(s)}(\bar{r})$. Suppose also that the scattered field is detected by a pair of coils connected in opposition. If $\bar{J}_\iota$ is the current density of coil ι, where $\iota = 1, 2$ then the induced emf V_ι in coil ι is given by

$$I_\iota V_\iota = -\int_{coil_\iota} \bar{E}^{(s)}(\bar{r}) \cdot \bar{J}_\iota(\bar{r}) d\bar{r} \qquad \iota = 1, 2 \tag{10}$$

This may also be expressed in a more compact notation as

$$I_\iota V_\iota = - < \bar{E}^{(s)} | \bar{J}_\iota > \qquad \iota = 1, 2 \tag{11}$$

Using the reciprocity principle we also have

$$I_\iota V_\iota = - < \bar{E}_\iota | \bar{P} > \qquad \iota = 1, 2 \tag{12}$$

where $\bar{E}_\iota$ is the field due to the source $\bar{J}_\iota$. Hence the differential probe response is given by
$$\begin{aligned} \Delta V &= V_1 - V_2 \\ &= - < \bar{e}_1 - \bar{e}_2 | \bar{P} > \\ &= -\int_{flaw} \Delta\bar{e}(\bar{r}) \cdot \bar{P}(\bar{r}) d\bar{r}, \qquad \iota = 1, 2 \end{aligned} \tag{13}$$

where $\bar{e}_\iota = \bar{E}_\iota/I_\iota$ and $\Delta\bar{e} = \bar{e}_1 - \bar{e}_2$. Transforming to a discrete form, $\bar{P}(\bar{r})$ is approximated by a pulse function sum using (3). Substituting the discrete approximation of the dipole density into our expression for the differential probe response, equation (13), and integrating over the volume elements gives

$$\Delta V = -\delta_x \delta_y \delta_z \sum_{k=0}^{N_x-1} \sum_{l=0}^{N_y-1} \sum_{m=0}^{N_z-1} \Delta\bar{e}_{klm} \cdot \bar{P}_{klm} \tag{14}$$

where

$$\Delta\bar{e}_{klm} = \int \Delta\bar{e}(\bar{r}) P_k(\frac{x}{\delta_x}) P_l(\frac{y}{\delta_y}) P_m(\frac{z-z_0}{\delta_z} - \frac{1}{2}) d\bar{r}. \tag{15}$$

NUMERICAL RESULTS

The flaw region, Figure 2, was discretized by dividing the slot into 64 elements along the length, 4 across the slot, and 8 layers. The elements are of equal size along each dimension, the number constrained to be powers of 2. This discretization gives 2048 volume elements. At each element our unknown is the electric current dipole moment, $\bar{P}$, which has three components. Therefore, the total number of unknowns in this discretized problem is 6144. The first stage of the solution involves calculating the matrix elements, taking advantage of the Toeplitz structure of the matrix to avoid repeated calculation of the same numerical result.

The matrix element calculations need to be carried out only once for a given set of mesh and electromagnetic parameters. The flaw shape can now be varied by changing the normalized conductivity of each volume element. This allows the study of various shaped defects inside the flaw region without recomputing the matrix.

The test piece (Figure 2) is made of austenitic steel type 18-10MO with a conductivity of $\sigma_0 = 1.7 \times 10^6$ S/m and a relative permeability $\mu_r = 1$. The inspection frequency was 500 Hz. The probe parameters shown in Figure 1 are now used in calculating two fields, one for the driving coil and one for the two sensing coils. These fields need only be computed once to get the response for any number of probe positions. We performed two scans, one perpendicular to the slot, the other parallel to it. The fields for the perpendicular scan took 160 CPU seconds (2.7 min)[1] to compute, while the fields for the parallel scan took twice as long partly because more points were considered.

The incident field from the driving coil, equation (8), is used as the right hand side of the linear system described by (5) and then solved for the unknowns, $\bar{P}_{klm}$, using a conjugate gradient algorithm. The resulting solution is now used in (14) to compute the differential voltage ΔV. A perpendicular scan can be performed by starting with the probe centered on the flaw and calculating the differential voltage at 1mm. increments through 40mm. total displacement. The results of such a numerical scan are presented in Figure 3. The axes are scaled by a constant term α, which depends on the product of the number of turns in the driving and sensing coils. It took approximately 120 CPU seconds to compute each point shown.

---

[1] All CPU times quoted are on a 10 MIP workstation using a 26 MFLOP array processor for implementing the FFTs.
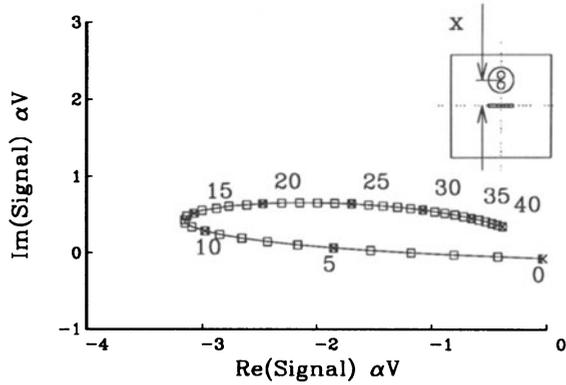
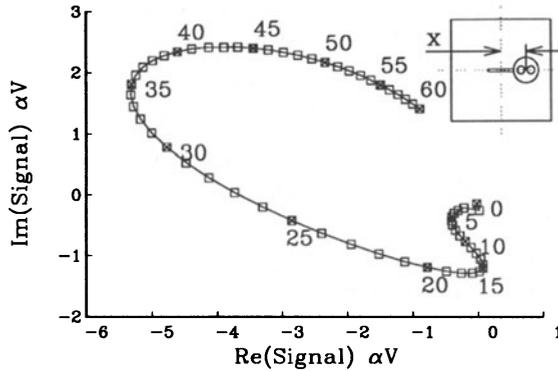Fig. 3.   Probe response for scan perpendicular to slot.

Fig. 4.   Probe response for scan parallel to slot.

Figure 4 shows the numerical results for a scan parallel to the slot. Again this scan started with the probe centered on the flaw and incremented the position 1mm. at a time through 60mm. It took approximately 250 CPU seconds to compute each point for this configuration.

Figure 5 compares the results of the differential voltage calculations with experimental data[4]. The experimental data available to the authors does not contain absolute phase information or absolute magnitude information, so the data has been normalized to (1,0) for the parallel scan results and (0,1) for the perpendicular case. The normalization point was chosen to be the point of maximum magnitude of signal. The experimental data shown was collected on a 30mm thick plate, 330mm long in the dimension of the slot length, 285mm in the dimension of the width[3]. The numerical results show reasonable agreement with the experimental results, even though the calculation assumes a half-space conductor. Because the skin depth ($\approx$ 17mm) is of the same magnitude as the slab thickness, reflection of the bottom surface of the slab cannot be neglected if accurate predictions are required. However, the half-space approximation gives a reasonable indication of the probe response.
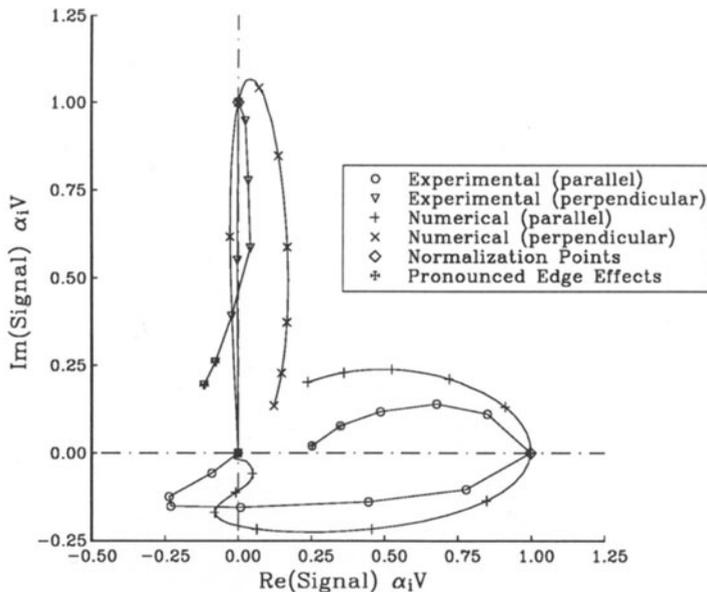
834

Fig. 5.   Comparison between experimental and numerical signals.

SUMMARY

We have demonstrated that the volume integral approach provides an efficient way of solving for the response of differential eddy-current probes over slots in half-spaces. The approach can be modified to solve for the response in finite slabs without any large computational overhead. The results compare favorably with experimental measurements.

REFERENCES

1. J. R. Bowler, L. D. Sabbagh and H. A. Sabbagh, <u>A Theoretical and Computational Model of Eddy-Current Probes Incorporating Volume Integral and Conjugate Gradient Methods</u> IEEE Trans. Magnetics Vol. 25, No.3, pp. 2650-2664 (1989).

2. L. R. Turner, Ed. <u>Proceedings of the Vancouver Team Workshop</u>, NTIS Report ANL/FPP/TM-230, 1988.

3. J. C. Verite, COMPEL, Vol. 3, No. 3, pp167-178, 1984.

4. J. C. Verite, A. Bossavit, J. Cahouet and Y. Crutzen, Eds. <u>Team Workshop and Meeting on the Applications of Eddy-Current Computations</u>, (Commission of European Communities, Brussels 1989).

5. R. F. Harrington, <u>Field Computations By Moment Methods,</u> (Macmillan, New York, 1968).

6. M. Hestenes, <u>Conjugate Direction Methods in Optimization</u>, (New York: Springer-Verlag, 1980).

7. J. R. Bowler, L. D. Sabbagh and H. A. Sabbagh, To be published.